Uncertain Darcy's problem and the stochastic particle transport

Giacomo Garegnani

Supervisors: Dr. Sebastian Krumscheid and Prof. Fabio Nobile

Contents

1 Expected exit time from a domain

We aim to estimate the exit time of a particle driven by a deterministic transport field and a stochastic diffusion from a domain $D \subset \mathbb{R}^d$. Given a vector $W(t)$ of m independent Brownian motions and two functions $f \colon \mathbb{R}^d \to \mathbb{R}^d, g \colon \mathbb{R}^d \to \mathbb{R}^{d \times m}$, we consider the following stochastic differential equation (SDE)

$$\begin{cases} dX(t) = f(X(t))dt + g(X(t))dW(t), & 0 < t \leq T, \\ X(0) = X_0, & X_0 \in D. \end{cases} \tag{1}$$

The problem is completed with two different types of boundary conditions, namely

   i. *killing boundaries*: if the particle exits D the process is stopped,

  ii. *reflecting boundaries*: the particle trajectory is reflected normally inside D when it touches the boundary ∂D.

Our aim is to estimate numerically the first exit time of the solution $X(t)$ from D, *i.e.*, the quantity

$$\tau = \min\{\min\{t \colon X(t) \notin D\}, T\}. \tag{2}$$

Let us remark that the parameter τ is meaningful only if there exists a portion of the boundary $\Gamma_k \subset \partial D$ that is endowed with killing boundary conditions. Otherwise, the process $X(t)$ will stay in D for the whole time interval, giving as a result $\tau = T$ for each realisation of $X(t)$. Another quantity of interest is defined as follows

$$\phi = \phi(T, X_0, F) = \mathbb{1}_{\{\tau < T\}} F(X(T)), \tag{3}$$

where $F \colon \mathbb{R}^d \to \mathbb{R}$ is a smooth function. An interesting choice of F could be the function mapping every x of $\mathbb{R}^d$ to the value 1. In this case, the expecation of ϕ is equal to the probability for $X(t)$ to exit the domain before the final time T. Let us choose the notation $F = 1$ in this case, getting

$$\Phi(T, X_0) = \mathbb{E}(\phi(T, X_0, 1)) = \Pr(\tau < T | X(0) = X_0) \tag{4}$$

In the case of general f, g and for a d-dimensional SDE, there is no closed form for τ and ϕ. Therefore, we approximate the value of τ by means of two numerical schemes, briefly presented in the following.

1.1 Numerical Methods

1.1.1 Discrete Euler-Maruyama

Given $N \in \mathbb{N}$ let us define a partition of $[0, T]$ as $P_h = \{t_i\}_{i=0}^N, t_i = ih, h = T/N$. The Discrete Euler-Maruyama method (DEM) for problem (1) is defined as follows

$$\begin{cases} X_h^d(t_{i+1}) = f(X(t_i))h + g(X(t_i))(W(t_{i+1}) - W(t_i)), \\ X_h^d(0) = X_0. \end{cases} \tag{5}$$

The exit time τ is approximated with the quantity τ_h^d defined as

$$\tau_h^d = \min\{\min\{t_i \colon X_h^d(t_i) \notin D\}, T\}. \tag{6}$$

We approximate analogously ϕ as

$$\phi_h^d = \mathbb{1}_{\{\tau_h^d < T\}} F(X_h^d(T)). \tag{7}$$

Let us state two results concerning the weak error of this method.

Proposition 1.1 *Under appropriate assumptions of smoothness of $f, g, D, \partial D, F$,*

$$|\mathbb{E}(\tau_h^d) - \mathbb{E}(\tau)| = O(\sqrt{h}). \tag{8}$$

Proposition 1.2 *Under approprate assumptions of smoothness of $f, g, D, \partial D, F$,*

$$|\mathbb{E}(\phi_h^d) - \mathbb{E}(\phi)| = O(\sqrt{h}). \tag{9}$$

An discussion of result 1.1 can be found in [5], its proof in [3]. A proof of 1.2 can be found in [1].

1.1.2 Continuous Euler-Maruyama.

Let us consider the partition P_h of $[0, T]$ as above. The Continuous Euler-Maruyama (CEM) method is defined as

$$\begin{cases} X_h^c(t) = f(X(t_i))(t - t_i) + g(X(t_i))(W(t) - W(t_i)), & t_i < t \le t_{i+1}, \\ X_h^c(0) = X_0. \end{cases} \tag{10}$$

Let us remark that in case the particle does not exit the domain, $X_h^c(t_i) = X_h^d(t_i)$ for all $t_i \in P_h$. It is possible to compute the probability that a particle has exited the domain at a time t between two consecutive timesteps t_i, t_{i+1} when D is an half-space with the following formula [2]

$$\Pr(\exists t \in [t_i, t_{i+1}] \quad X_h^d(t) \notin D | X_h^d(t_i) = x_i, X_h^d(t_{i+1}) = x_{i+1}) = p(x_i, x_{i+1}, h), \tag{11}$$

with $p(x_i, x_{i+1}, h)$ given by

$$p(x_i, x_{i+1}, h) = \exp\left(-2\frac{[n \cdot (x_i - z_i)][n \cdot (x_{i+1} - z_i)]}{hn \cdot (gg^T(x_i)n)}\right), \tag{12}$$

where z_i is the projection of x_i on ∂D and n is the normal to ∂D in z_i. At each timestep t_{i+1} we compute the probability $p(x_i, x_{i+1}, h)$, and then simulate a variable U distributed uniformly in the interval $[0, 1]$, thus obtaining a realization u. Hence, we counclude that the particle has left the domain for a time t in (t_i, t_{i+1}) if u is smaller than p. Therefore, we approximate the exit time as

$$\tau_h^c = \min\{T, \min\{t_i = hi\colon X_h(t_i) \notin D\}, \min\{t_i = hi\colon u < p(x_{i-1}, x_i, h)\}\}, \tag{13}$$

In the same way as in DEM, we can approximate ϕ as

$$\phi_h^c = \mathbb{1}_{\{\tau_h^c < T\}} F(X_h^c(T)). \tag{14}$$

We show the pseudocode for the implementation of CEM in Algorithm 1.
The weak error of this method has been studied exhaustively in previous work.

Proposition 1.3 *Under appropriate smoothness assumptions,*

$$|\mathbb{E}(\phi_h^c) - \mathbb{E}(\phi)| = O(h). \tag{15}$$

A proof of result 1.3 can be found in [2].

Algorithm 1: Continuous Euler-Maruyama

> **for** $t_i \in P_h$ **do**
> > $X(t_{i+1}) = f(X(t_i))h + g(X(t_i))(W(t_{i+1}) - W(t_i))$;
> > **if** $X(t_{i+1}) \notin D$ **then**
> > > $\tau_h^c = t_{i+1}$;
> > > $\phi_h^c = F(X_h^c(t_{i+1}))$;
> > > **return**;
> >
> > **else**
> > > compute $p = p(x_i, x_{i+1}, h)$;
> > > simulate $u \sim \text{Unif}(0,1)$;
> > > **if** $u < p$ **then**
> > > > $\tau_h^c = t_{i+1}$;
> > > > $\phi_h^c = F(X_h^c(t_{i+1}))$;
> > > > **return**;
> > >
> > > **end**
> >
> > **end**
>
> **end**

1.1.3 Reflecting boundaries

The reflecting boundaries are treated in the same way for both DEM and CEM. Let us denote by Γ_k and Γ_r the killing and reflecting subsets of ∂D, *i.e.*

$$\Gamma_r \cup \Gamma_k = \partial D, \quad \Gamma_r \cap \Gamma_k = \emptyset \tag{16}$$

In case the particle approaches Γ_k the exit is treated as above. If for a timestep of $t_i \in P_h$, $X(t_i)$ is not in D and has crossed Γ_r at a time $t_{i-1} < t < t_i$, we update the solution to be the normal reflection inside D of $X(t_i)$.

1.1.4 An adaptive procedure

Let us consider the function g in (1) to be fixed to a real constant σ. The numerical methods we presented can be completed with an adaptive procedure for the step size h. In this frame, adaptivity is performed with respect to the position of the numerical solution $X_h(t_i)$, *i.e.*, the step size is reduced if the solution is near to the boundary of the domain D. If we denote by d_i the distance between $X_h(t_i)$ and its normal projection on ∂D, by $l \in \mathbb{N}$ a fixed parameter and by h_0 a maximum bound for h, the step size is chosen using the following formula

$$h = \max\left\{2^{-2l}h_0, \min\left\{2^{-l}h_0, \left(\frac{d}{(l+3)\sigma}\right)^2\right\}\right\}. \tag{17}$$

This formula is equivalent to dividing the domain D in three zones, in particular

- an interior zone where $h = h_{int} = 2^{-l}h_0$,

- a boundary zone where $h = h_{bound} = 2^{-2l}h_0$,

- an intermediate zone where $h = \frac{d}{(l+3)\sigma}^2$.

Since the loss of 0.5 in the weak order of convergence of Euler-Maruyama is due to the non-detected exits from the domain D, refining the step size only near to the boundary could lead to an error equal to the one obtained using h_{bound} on the whole domain.

1.2 A PDE approach

It is possible to express the mean exit time and the probability of exit from a domain in terms of the solution of partial differential equations (PDE's). Let us denote by Γ_k, Γ_r the killing and reflecting subsets of ∂D. We consider then the expectation of the exit time from the domain D for a trajectory that at $t = 0$ is at position x, *i.e.*,

$$\bar{\tau}(x) = \mathbb{E}(\tau | X(0) = x). \tag{18}$$

Let us define the operator $\mathcal{L}$ induced by (1) acts on a function $u \colon \mathbb{R}^d \to \mathbb{R}$ as follows

$$\mathcal{L}u = f \cdot \nabla u + \frac{1}{2} g g^T : \nabla \nabla u, \tag{19}$$

where the $:$ operator between two matrices A, B in $\mathbb{R}^{d \times d}$ is defined as follows

$$A : B = \sum_{i,j=1}^{d} \{A\}_{ij} \{B\}_{ij} = \mathrm{tr}(A^T B). \tag{20}$$

The following result allows computing the mean exit time as the solution of an appropriate PDE.

Proposition 1.4 *Let $\mathcal{L}$ be the differential operator defined as (19). Then, if Γ_k and Γ_r are respectively the killing and reflecting subsets of ∂D, such that $\Gamma_k \cup \Gamma_r = \partial D, \Gamma_k \cap \Gamma_r = \emptyset$, the mean exit time $\bar{\tau}(x)$ for the solution $X(t)$ of (1) with $X_0 = x$ is the solution of the following boundary value problem*

$$\begin{cases} \mathcal{L}\bar{\tau}(x) = -1, & in \ D, \\ \bar{\tau}(x) = 0, & on \ \Gamma_k, \\ \nabla \bar{\tau}(x) \cdot n = 0, & on \ \Gamma_r, \end{cases} \tag{21}$$

where n is the normal to Γ_r.

Further analytical treatement of the mean exit time can be found in [6, 8].

We now consider the probability of exit from D for a solution $X(t)$ that is equal to x for $t = s < T$. This probability is the solution of a boundary value problem.

Proposition 1.5 *Let $\mathcal{L}$ be the differential operator defined as (19). Then, if Γ_k and Γ_r are respectively the killing and reflecting subsets of ∂D, such that $\Gamma_k \cup \Gamma_r = \partial D, \Gamma_k \cap \Gamma_r = \emptyset$*

$$\Pr(\tau < T | X(s) = x) = \Phi(x, s, T) \tag{22}$$

where $\Phi(x, t, T)$ is the solution of the following backwards PDE

$$\begin{cases} \dfrac{\partial}{\partial t} \Phi(x, t, T) + \mathcal{L}\Phi(x, t, T) = 0 & in \ D, s \leq t < T, \\ \Phi(x, t, T) = 1 & on \ \Gamma_k, s \leq t \leq T, \\ \nabla \Phi(x, t, T) \cdot n = 0, & on \ \Gamma_r, s \leq t \leq T, \\ \Phi(x, T, T) = 0 & in \ D, \end{cases} \tag{23}$$

where n is the normal to Γ_r.

The proof in case $\Gamma_k = \partial D$ of this result can be found in [9]. Further treatment in case of mixed boundary conditions and the closed form of the solution for some particular geometries of $D \subset \mathbb{R}^2$ can be found in [4]. It is therefore possible to approximate $\bar{\tau}$ and Φ by means of classical methods for solving PDE's numerically, such as finite differences or the Finite Elements Method.

1.3 One-Dimensional Case

We consider problem (1) in case $d = 1$. Given $f, g \colon \mathbb{R} \to \mathbb{R}$, an interval $D = [l, r]$ and a Brownian motion $W(t)$, let us consider the following one dimensional SDE

$$\begin{cases} dX(t) = f(X(t))dt + g(X(t))dW(t), & 0 < t \leq T, \\ X(0) = X_0, & X_0 \in D. \end{cases} \tag{24}$$

In this case, the boundary of D consists of the two points $\{l, r\}$. In order for the problem of the determination of τ to be meaningful, at least one of the two points should be endowed with a killing boundary condition.

1.3.1 Analytical expression of the mean exit time

In this simple frame, it is possible to deduce an analytical solution $\bar{\tau}$ of (21). Let us consider the boundary condition at $x = l$ fixed as *killing* and vary the boundary condition at $x = r$. Since the scope is deducing the exit time of a particle from D, this assumption is plausible. In this frame, it is possible to rewrite (21) as

$$\begin{cases} f(x)\bar{\tau}'(x) + \dfrac{1}{2}g^2(x)\bar{\tau}''(x) = -1, & l < x < r, \\ \bar{\tau}(l) = 0, & \\ \bar{\tau}(r) = 0, & \text{if for } x = r \text{ the boundary is } killing, \\ \bar{\tau}'(r) = 0, & \text{if for } x = r \text{ the boundary is } reflecting. \end{cases} \tag{25}$$

It is possible to show [6, 8] that $\bar{\tau}$ is in the one-dimensional case given by

$$\bar{\tau}(x) = -2 \int_l^x \exp(-\psi(z)) \int_l^z \frac{\exp(\psi(y))}{g^2(y)} dy + c_1 \int_l^x \exp(-\psi(y)) dy + c_2, \tag{26}$$

where the function ψ is defined as

$$\psi(x) = \int_l^x \frac{2f(y)}{g^2(y)} dy, \tag{27}$$

and the constants $c_1, c_2 \in \mathbb{R}$ depend on the boundary conditions as follows

$$\begin{aligned} & c_1 = 2\frac{\int_l^r \exp(-\psi(z)) \int_l^z \frac{\exp(\psi(y))}{g^2(y)} dy}{\int_l^r \exp(-\psi(y)) dy}, \quad \text{if for } x = r \text{ the boundary is } killing, \\ & c_1 = 2 \int_l^r \frac{\exp(-\psi(y))}{g(y)^2} dy, \quad \text{if for } x = r \text{ the boundary is } reflecting, \\ & c_2 = 0. \end{aligned} \tag{28}$$

Let us remark that in case $f = -V'$ for some smooth function V and $g = \sigma \in \mathbb{R}$, the expression of ψ semplifies to

$$\psi(x) = 2\frac{V(l) - V(x)}{\sigma^2}. \tag{29}$$

The value for the expected exit time given by (26) will be used as a reference for verifying the order of convergence of the numerical methods.
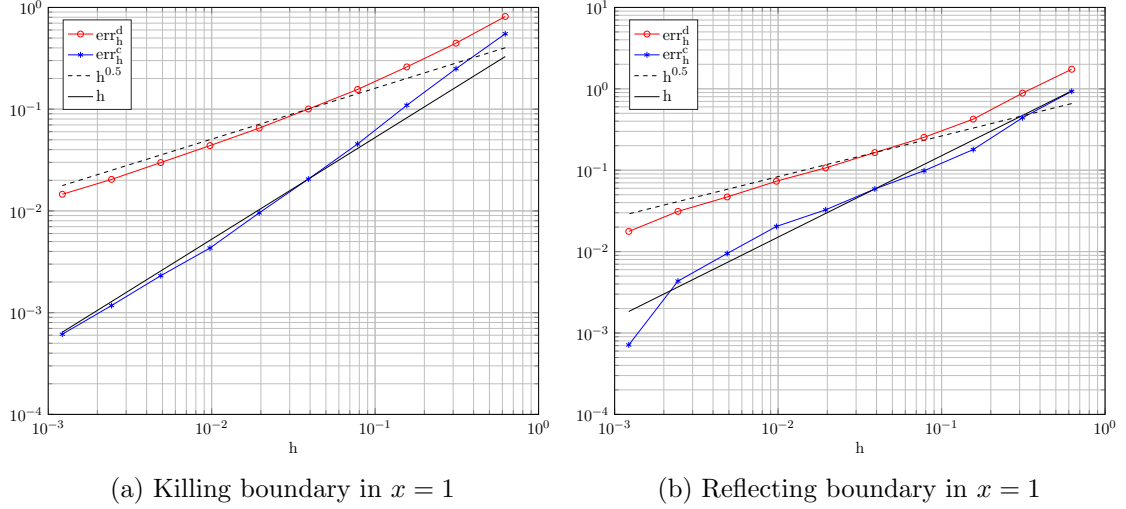
(a) Killing boundary in $x = 1$ (b) Reflecting boundary in $x = 1$

Figure 1: Approximation of τ. Orders of convergence for DEM and CEM in the one-dimensional case.

1.3.2 Numerical experiments - Estimation of τ

Smooth case. We consider as a domain for (24) the interval $D = [-1, 1]$, final time $T = 5$ and the following functions

$$f(x) = -V'(x), \text{ where } V(x) = 0.1(8x^4 - 8x^2 + x + 2),$$
$$g(x) = \sigma = 3. \tag{30}$$

We approximate the value of τ with a Montecarlo simulation of τ_h^d and τ_h^c computed as in (6) and (13) from the solutions provided by DEM and CEM respectively. In order to verify the order of convergence of the methods, we let N vary in the set $2^i, i = 3, \ldots, 12$ and we fix the number of trajectories M to 10000. In this way, the error caused by the Montecarlo estimation should not spoil the order of convergence. In Figure 1 we show the errors obtained fixing $X_0 = 0$ in both the cases of killing and reflecting boundary conditions in $x = 1$. Moreover, in Figure 2 we show an approximation of τ obtained with the two methods with $h = T/128$ and $M = 1000$ for a set of 10 initial values equispaced along D. It is possible to remark that computing the probability of exit between two consecutive timesteps as in (12) allows correcting the overestimation of τ obtained simply using DEM. We want to estimate the computational time for both the method. We consider $M = 10000$, killing boundary conditions and $N = 2^i, i = 3, \ldots, 12$. It is possible to remark in Figure 3 that the computational time required by CEM is higher than for DEM if the same value of h is employed. On the other hand, fixing the error, CEM is faster than DEM in this case.

Rough case. We consider the same domain D as above, $T = 5$ and $g = \sigma = 3$. We consider V to be piecewise linear, so that $f = -dV$ is piecewise constant. In particular, we choose the following form for V

$$V = 0.1 \begin{cases} -2x - 1, & x < -0.5, \\ 4x + 2, & -0.5 \leq x < 0, \\ -2x + 2, & 0 \leq x < 0.5, \\ 4x - 1, & x \geq 0.5. \end{cases} \tag{31}$$
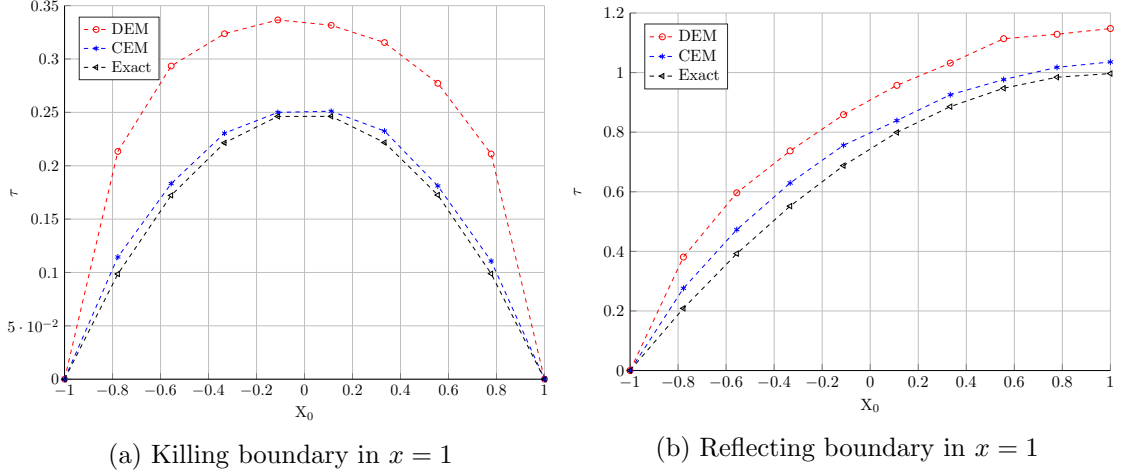
7

(a) Killing boundary in $x = 1$ (b) Reflecting boundary in $x = 1$

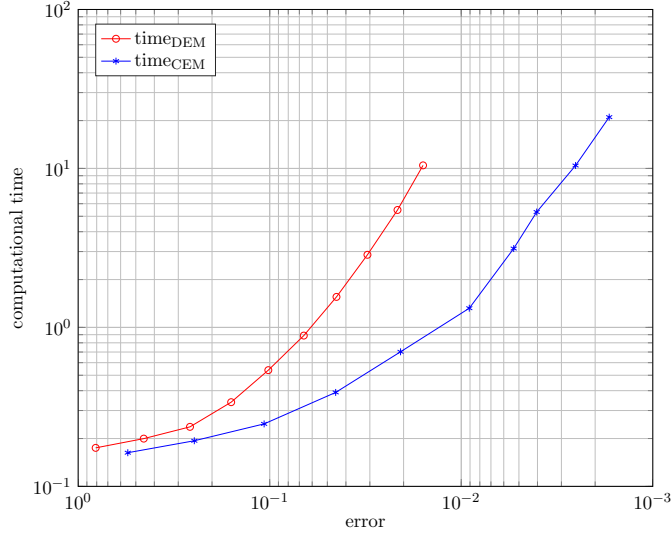Figure 2: Approximation of τ as a function of the initial value X_0.

Figure 3: error vs work plot for DEM and CEM.

This is a linear interpolation of the function V we used in the smooth case above in the points $\{-1, -0.5, 0, 0.5, 1\}$ (Figure 4). This case is of particular interest, since if the function f is the result of a numerical method on a PDE, it could not be smooth as in the previous case. We perform DEM and CEM with the same parameters as before, *i.e.*, $M = 10000, N = 2^i, i = 3, \ldots, 12$. In Figure 5 it is possible to remark that the rate of convergence of DEM is unvaried with respect to the previous case. The CEM method experiences a slight decrease in the order of convergence with respect to the smooth case.

1.3.3 Numerical approximation of Φ with the PDE approach

Let us consider D as the interval $[l, r]$, the boundary condition in l to be fixed to killing and in r to be either killing or reflecting. In this case and for f independent of t and
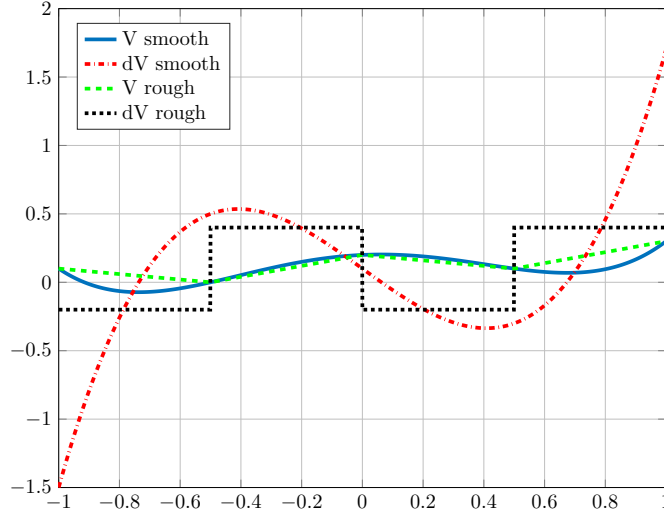
8

Figure 4: V and dV employed in the numerical experiments in both the smooth and rough cases.

$g = \sigma \in \mathbb{R}$ (23) can be written as the following initial value PDE

$$
\begin{cases}
-\dfrac{\partial}{\partial t}\Phi(t,x) + f\dfrac{\partial}{\partial x}\Phi(t,x) + \dfrac{1}{2}\sigma^2\dfrac{\partial^2}{\partial x^2}\Phi(t,x) = 0, & l < x < r \\[2mm]
\Phi(t,l) = 1, & \\[2mm]
\Phi(t,r) = 1, & \text{if for } x = r \text{ the boundary is } \textit{killing} \\[2mm]
\dfrac{\partial}{\partial x}\Phi(t,r) = 0, & \text{if for } x = r \text{ the boundary is } \textit{reflecting} \\[2mm]
\Phi(0,x) = 0. &
\end{cases}
$$

(32)

This equation can be solved, *e.g.*, using finite differences. We employ the theta method for solving (32). Let us consider the case in which r is a killing boundary, *i.e.*, the PDE is endowed with Dirichlet boundary conditions. Given a step size Δ_t for time integration and an uniform grid $x_i = l + i\Delta_x, i = 0, \ldots, N+1, x_{N+1} = r$, at each timestep k one has to find the solution of the linear system

$$
(I - \Delta_t\theta A)u^{k+1} = (I + \Delta_t(1-\theta)A)u^k + hF,\ 0 \le \theta \le 1,
$$

(33)

where I is the identity matrix of $\mathbb{R}^{N\times N}$. The matrix A of $\mathbb{R}^{N\times N}$ and the vector F of $\mathbb{R}^N$ define the space discretization and the boundary conditions and are defined by

$$
A = \frac{1}{2\Delta_x}\begin{pmatrix} \alpha_1 & \beta_1 & \\ \gamma_1 & \alpha_2 & \beta_2 \\ & \ddots & \ddots & \ddots \end{pmatrix}, \quad F = \frac{1}{2\Delta_x}\left(F_1 \cdots F_N\right)^T
$$

(34)

(a) Killing boundary in $x = 1$ (b) Reflecting boundary in $x = 1$
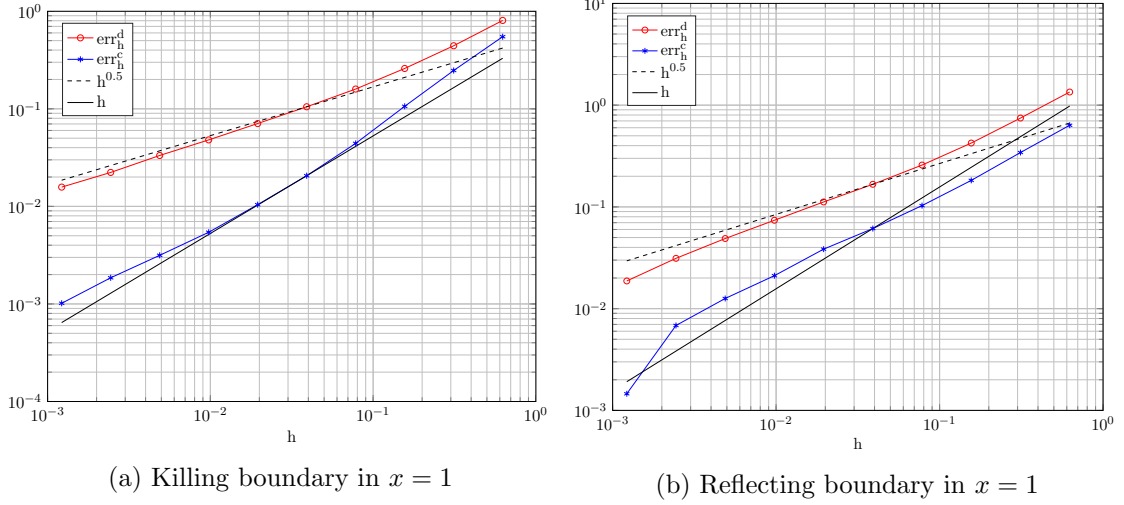
Figure 5: Approximation of τ. Orders of convergence for DEM and CEM in the one-dimensional case with f piecewise constant.

and the coefficients are given by

$$
\begin{aligned}
\alpha_i &= -\frac{2\sigma^2}{\Delta_x}, \ i = 1, \ldots, N, \\
\beta_i &= \frac{\sigma^2}{\Delta_x} + f(x_i), \ i = 1, \ldots, N-1, \\
\gamma_i &= \frac{\sigma^2}{\Delta_x} - f(x_{i+1}), \ i = 1, \ldots, N-1, \\
F_1 &= \frac{\sigma^2}{\Delta_x} - f(x_1), \\
F_N &= \frac{\sigma^2}{\Delta_x} - f(x_{N-1}).
\end{aligned}
\tag{35}
$$

The case of reflecting boundary condtion in $x = r$ is similar and affects only the computation of the matrix A and the vector F. In particular, we introduce a *ghost node* at position $x = r + \Delta_x$, compute the derivative using a centrate approximation and impose that it is equal to 0, which leads to the condition that the value in the node in $x = r$ is equal to the value in $x = r - \Delta_x$. Since the matrix defining the system (33) is tridiagonal, one can choose Δ_t, Δ_x to be small and obtain a precise solution of (32) in a reasonable computational time. In the following, we will compare the values given by Montecarlo simulations using DEM and CEM with the solution of the theta method with $\theta = 0.5$.

1.3.4 Numerical experiments - Estimation of Φ

Smooth case. We consider (24) with $D = [-1, 1]$, the final time $T = 0.5$ and we define

$$
\begin{aligned}
f(x) &= -V'(x), \text{ where } V(x) = 8x^4 - 8x^2 + x + 2, \\
g(x) &= \sigma = 2.
\end{aligned}
\tag{36}
$$

In order to approximate Φ, we perform a Montecarlo simulation using both DEM and CEM, with $M = 6 \cdot 10^5$ trajectories in order to kill the statistical error. We consider the number of timesteps for the time integration to be $N = 2^i, i = 5, \ldots, 12$. Numerical results
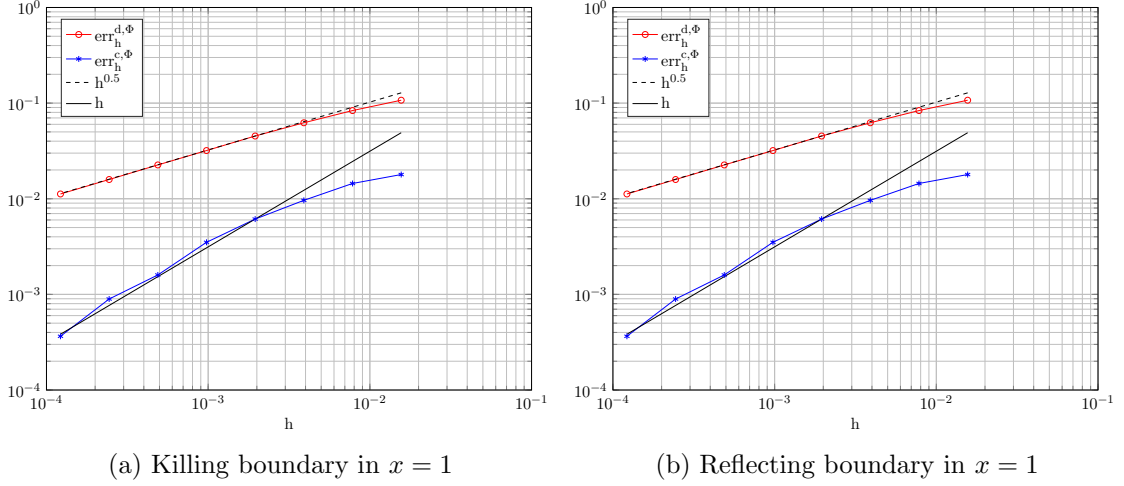
(a) Killing boundary in $x = 1$ (b) Reflecting boundary in $x = 1$

Figure 6: Approximation of Φ. Orders of convergence of DEM and CEM in the one-dimensional case.

(Figure 6a) confirm that the weak error for DEM is of order 0.5, while for CEM the order of convergence is 1.

1.4 Two-dimensional case

We are interested in estimating the exit time of a particle from a domain $D \subset \mathbb{R}^2$. Given $W(t)$ a vector of two independent Brownian motions, we consider the equation (1). In this case, $f \colon \mathbb{R}^2 \to \mathbb{R}^2, g \colon \mathbb{R}^2 \to \mathbb{R}^{2 \times 2}$. We compute the mean exit time and the exit probability using DEM and CEM and compare results with the numerical solution of the PDE's presented in 1.2.

### 1.4.1 Numerical experiments - Estimation of τ

Killing boundary conditions. We consider a simple case of (1) in $D = [-1, 1] \times [-1, 1]$, where

$$f = 0 \in R^2, \ g = \sigma I \in R^{2 \times 2}, \sigma \in \mathbb{R}.$$

Moreover, we consider ∂D to be a killing boundary. The solution in this case is a Brownian motion. In this case, the partial differential equation (21) reduces to

$$\begin{cases} -\sigma^2 \Delta \bar{\tau} = 2, & \text{in } D, \\ \quad\quad \bar{\tau} = 0, & \text{on } \partial D. \end{cases} \tag{37}$$

This is the Poisson equation, hence it is possible to solve it numerically with the Finite Elements Method or the finite differences avoiding a high computational cost. We use the Finite Elements Method adopting a regular mesh with equal constant spacing in the x and y directions, obtaining a solution as in Figure 7b. In order to verify the orders of convergence of DEM and CEM, we set $T = 3$, $\sigma = 1$, $X_0 = (0, 0)^T$, with $M = 10000$ and $N = 2^i, i = 3, \ldots, 9$. We then compare the Montecarlo estimation we obtain with the value of $\bar{\tau}$ in $(0, 0)$, obtained by interpolation on the Finite Elements solution. The orders of convergence for this numerical experiment are shown in Figure 7a. The results confirm the theoretical orders of convergence for DEM and CEM, with an average order of 0.55 for DEM and 0.93 for CEM, which corrects to 0.98 if the last point is not taken into account.
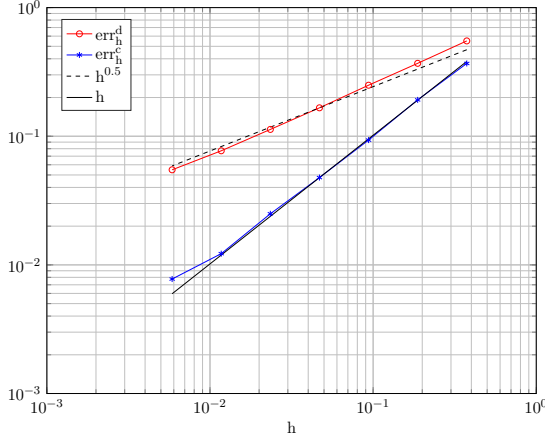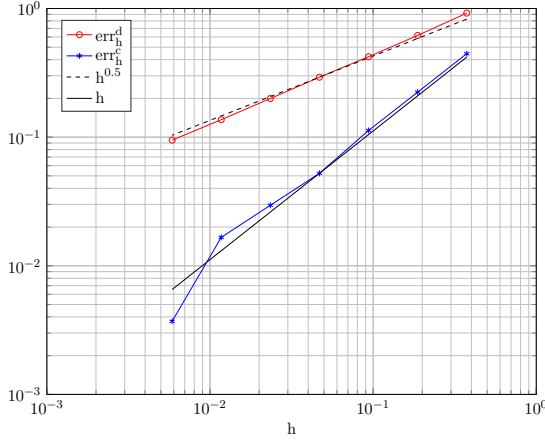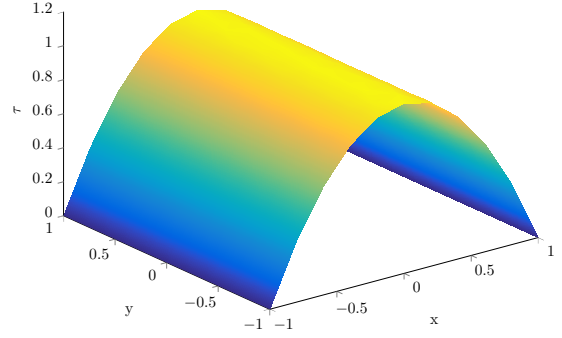
(a) Convergence of CEM and DEM.
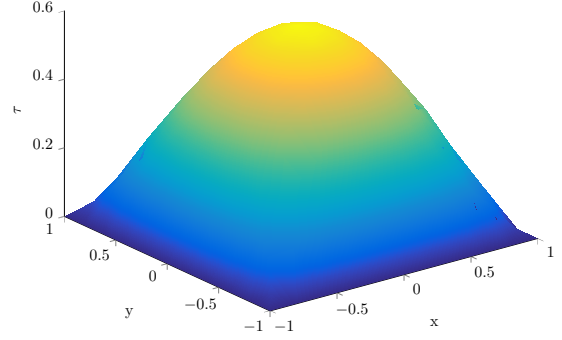
(b) Expectation of exit time.

Figure 7: Summary of the results for τ in the two-dimensional case with pure killing boundary conditions.

(a) Convergence of CEM and DEM.

(b) Expectation of exit time.

Figure 8: Summary of the results for τ in the two-dimensional case with mixed boundary conditions.

Mixed boundary conditions. We consider the same problem as above with mixed killing and reflecting boundary conditions. f and g are the same as above, so the SDE model does not change, but we consider the two left and right boundaries of D, defined by $x = \pm 1$, to be reflecting. We denote this portion of the boundary as Γ_r, and the rest as Γ_k. In this case, the equation for $\bar{\tau}$ becomes

$$\begin{cases} -\sigma^2 \Delta \bar{\tau} = 2, & \text{in } D, \\ \bar{\tau} = 0, & \text{on } \Gamma_k, \\ \partial \bar{\tau} \cdot n = 0, & \text{on } \Gamma_r. \end{cases} \tag{38}$$

The solution of this equation is shown in Figure 8b. We compute the expectation of τ with DEM and CEM with the same parameters as above. The results (Figure 8a), show that the theoretical orders of convergence are not spoilt by this choice of boundary conditions. The mean order for DEM in this case is 0.55, while for CEM it is 1.15.
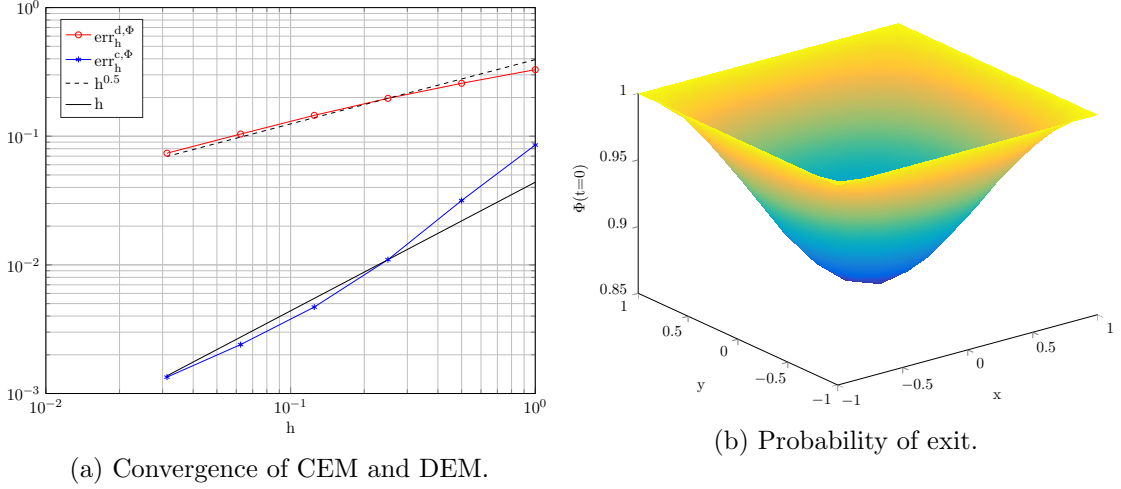
(a) Convergence of CEM and DEM.

(b) Probability of exit.

Figure 9: Summary of the results for Φ in the two-dimensional case with pure killing boundary conditions.

1.4.2 Numerical experiments - Estimation of Φ

Killing boundary conditions. We consider the same simple case as in section 1.4.1 We consider ∂D to be a killing boundary. The solution of (1) is in this case a Brownian motion. In this case, the partial differential equation (23) reduces to

$$\begin{cases} \dfrac{\partial}{\partial t}\Phi(x,t,T) + \dfrac{1}{2}\sigma^2\Delta\Phi(x,t,T) = 0, & \text{in } D, 0 \le t < T, \\ \qquad\qquad\qquad \Phi(x,t,T) = 1, & \text{on } \partial D, 0 \le t < T, \\ \qquad\qquad\qquad \Phi(x,T,T) = 0, & \text{in } D. \end{cases} \tag{39}$$

We solve this problem numerically with the Finite Elements Method as for (38). The solution at $t = 0$ is shown in Figure 9b. We verify the orders of convergence of DEM and CEM setting $X_0 = (0,0)^T, \sigma = 1, T = 1$. We consider $M = 100000$ trajectories and $N = 2^i, i = 0,\ldots,5$. We then compare the Montecarlo estimation with the value of Φ in $(0,0)$, obtained by interpolation on the Finite Elements solution. The orders of convergence for this numerical experiment are shown in Figure 9a. The theoretical orders of convergence are confirmed in this case as well, with an average order of 0.43 for DEM and 1.19 for CEM.

Mixed boundary conditions. We consider the same values for the parameters, the time integration and the Montecarlo estimation as in the pure killing case. In this case, we set the boundary conditions to be reflecting on the subset of the boundary of D defined by $x = \pm 1$ and killing for the other boundaries. Therefore, in this case the exit probability Φ is the solution of the folllowing PDE

$$\begin{cases} \dfrac{\partial}{\partial t}\Phi(x,t,T) + \dfrac{1}{2}\sigma^2\Delta\Phi(x,t,T) = 0, & \text{in } D, 0 \le t < T, \\ \qquad\qquad\qquad \Phi(x,t,T) = 1, & \text{on } \Gamma_k, 0 \le t < T, \\ \qquad\qquad \nabla\Phi(x,t,T)\cdot n = 0, & \text{on } \Gamma_r, 0 \le t < T, \\ \qquad\qquad\qquad \Phi(x,T,T) = 0, & \text{in } D. \end{cases} \tag{40}$$

The solution of this equation computed with Finite Elements is shown in Figure 10b. The convergence results for DEM and CEM are shown in Figure 10a. The mean orders in

13
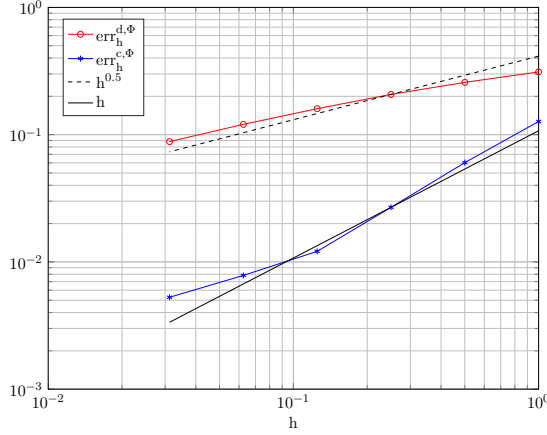
(a) Convergence of CEM and DEM.
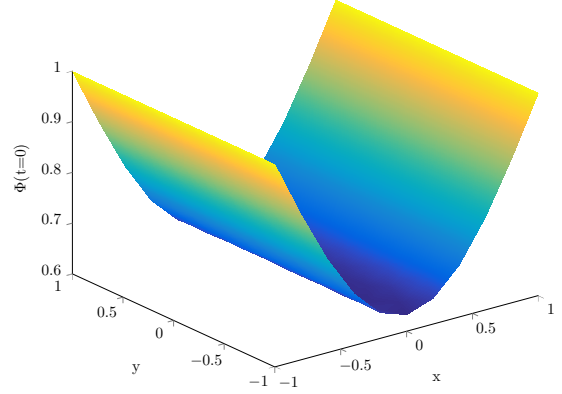
(b) Probability of exit.

Figure 10: Summary of the results for Φ in the two-dimensional case with mixed boundary conditions.

this case are 0.37 for DEM and 0.87 for CEM, which is less than the prediction given by theoretical results. This decrease in the convergence rate is remarkable for small values of h. This could mean that the error caused by the Finite Element approximation of the solution of (40) is not negligible with respect to the error of CEM.

1.4.3 Numerical experiments - Adaptivity

We apply to a test case the adaptivity procedure explained in section 1.1.4. In particular, we fix $f = 0, g = \sigma = 2, T = 10$ and $X_0 = (0,0)^T$ in the square domain $[0,1]^2$ with mixed boundary conditions. We vary the parameter l in (17) and we run DEM algorithm with $h = h_{bound}$ for all time steps and DEM with the adaptive procedure, in order to observe the convergence of the algorithm. We expect that either choosing only the finer step size for the whole solution or using the adaptivity procedure, we will observe that the error with respect to the reference solution will be $O(h_{int})$. However, since in the interior zone of the domain D the step size is bigger for the adaptive method, we expect the computational cost to be smaller than for the normal DEM. Therefore, we perform a Montecarlo simulation over $M = 10000$ trajectories, fixing $h_0 = T$ and $l = 4, \ldots, 8$. We estimate the mean exit time $\bar{\tau}$ comparing it with the solution of (38). In order to measure the computational cost, we compute the average over the whole set of trajectories of the number of Euler-Maruyama steps that are performed. In Figure 11 it is possible to remark that using a wider step in the center of the domain does not spoil the order of convergence of the method while reducing the number of iterations needed to estimate the mean exit time in a non-negligible manner, especially for smaller values of the step size.

2 The uncertain Darcy problem

The two methods for approximating the mean exit time have been investigated in a general frame. In the following we will consider (1) with $f \colon \mathbb{R}^2 \to \mathbb{R}^2$ given by the solution of the uncertain Darcy problem.
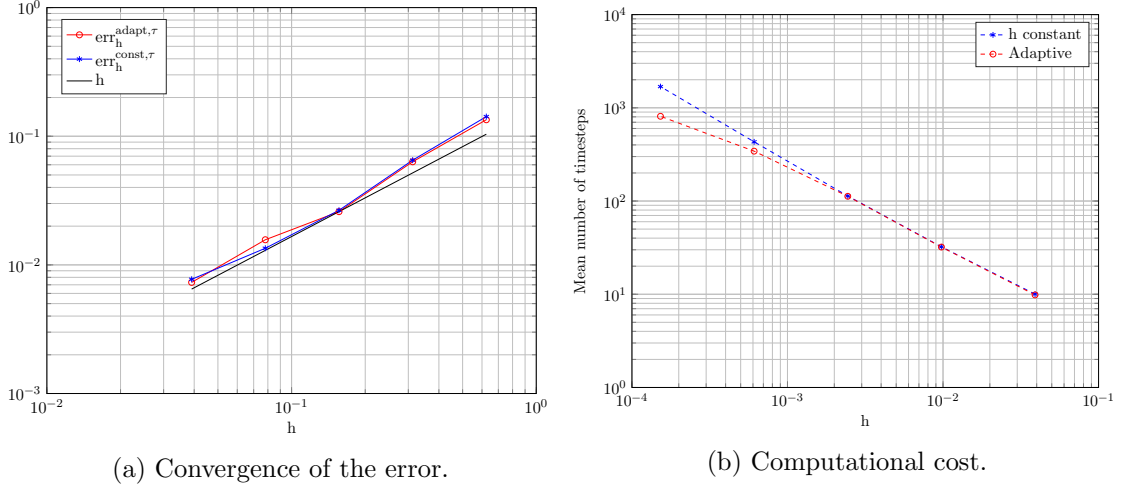
(a) Convergence of the error.

(b) Computational cost.

Figure 11: Estimation of τ in the square domain with mixed boundary conditions. Comparison between DEM with fixed or adaptive step size.

2.1 Problem statement

Let us consider a domain $D \subset \mathbb{R}^2$. Let us define the Neumann boundaries of D as Γ_N, its inlet boundary as Γ_{in} and its outlet boundary as Γ_{out}. Then, we search the solution of the following problem

$$
\begin{cases}
u = -A\nabla p, & \text{in } D, \\
\nabla \cdot u = 0, & \text{in } D, \\
p = p_0, & \text{on } \Gamma_{in}, \\
p = 0, & \text{on } \Gamma_{out}, \\
\nabla p = 0, & \text{on } \Gamma_N,
\end{cases}
\tag{41}
$$

where A is a random field. The solution u of this equation is used as transport field in equation (1), which can be therefore written as

$$
\begin{cases}
dX(t) = u(X)dt + \sigma dW(t), & 0 < t \leq T, \\
X(0) = X_0, & X_0 \in D,
\end{cases}
\tag{42}
$$

where we set the boundary conditions to be reflecting on Γ_N and killing on both $\Gamma_{in}, \Gamma_{out}$.

2.2 Finite Elements solution of the Darcy problem

Let us consider the domain $D = [-1,1] \times [-1,1]$. The random field A in (41) is chosen to be lognormal, *i.e.*,

$$
A = e^\gamma,
\tag{43}
$$

where γ is a normal random field defined by its covariance function $\text{cov}_\gamma(x_1, x_2)$ for any couple of points x_1, x_2 in the domain D. The covariance function is of the Matern family, thus having the following form

$$
\text{cov}_\gamma(x_1, x_2) = \frac{\sigma_A^2}{\Gamma(\nu)2^{\nu-1}} \left(\sqrt{2\nu} \frac{|x_1 - x_2|}{L_c} \right)^\nu K_\nu \left(\sqrt{2\nu} \frac{|x_1 - x_2|}{L_c} \right), \quad \nu \geq 0.5,
\tag{44}
$$

where σ_A^2 is the variance, L_c is the correlation length, Γ is the gamma function, K_ν is the modified Bessel function of the second kind and ν is a parameter. Let us remark that

15

(a) Random field.

(b) Pressure field.

(c) x component of velocity field.

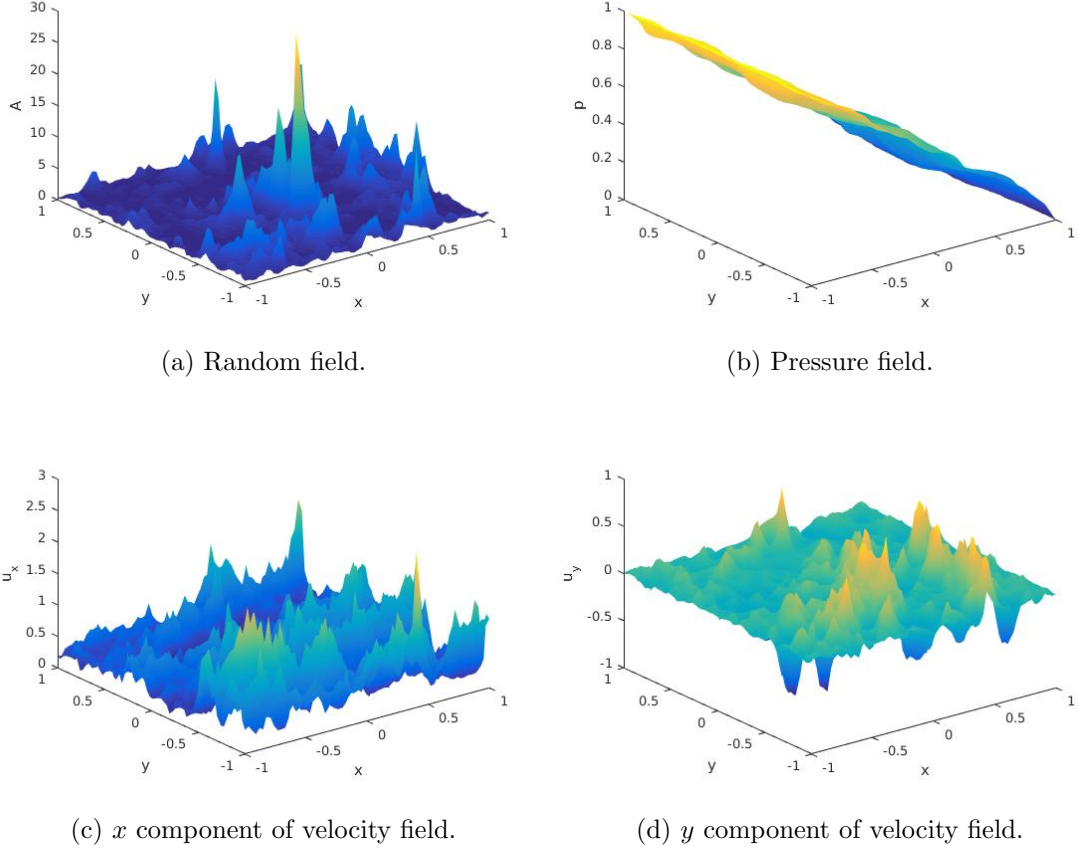(d) y component of velocity field.

Figure 12: Approximate solution of the uncertain Darcy problem.

the covariance function does not depend on x_1, x_2 but only on their euclidean distance $|x_1 - x_2|$. The regularity of the covariance function and of the realizations of A depend on ν. In particular, for ν equal to 0.5, the covariance is Lipschitz continuous and the field is α-Hölder continuous for $\alpha < 0.5$. Results concerning further regularity properties of A can be found in [7]. The realizations of A are computed using a discrete Fourier transformation on the vertices of a grid of D, equispaced on both the x and y directions with the same spacing Δ_A. Then, the numerical solution p_h of (41) is obtained with linear Finite Elements on a regular mesh T_p with maximum element size Δ_p. Since the vertices of the grid on which we compute A do not coincide with the vertices of T_p, we interpolate A on T_p to obtain p_h. Then, the velocity field u_h is retrived computing the gradient of p_h. The results for a realization of A are shown in Figure 12, where the value of the inlet pressure p_0 is equal to 1, and the parameters for the random field are $\nu = 0.5, L_c = 0.05$.

2.3 Solution of the SDE

Once the Finite Element approximation u_h of the velocity field is available, it is possible to approximate by means of DEM and CEM the solution of (42). The values of the numerical solution X_h can take any value in D, therefore it is necessary that the velocity field is defined in any point in D. If an interpolation of u_h is performed at each step, both DEM and CEM lose in computational efficiency. Hence, an interpolation of u_h has
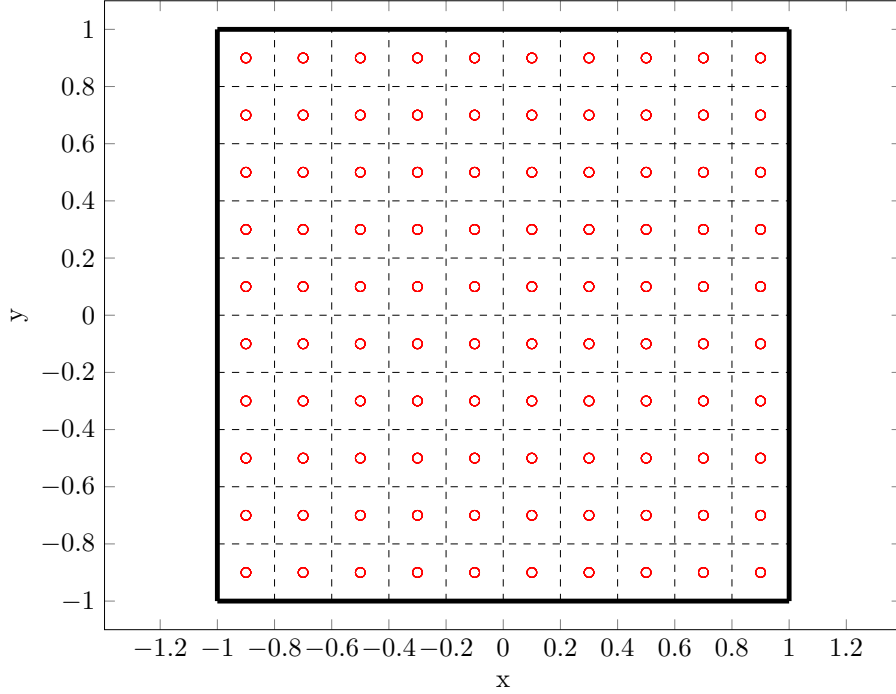
Figure 13: Grid used for interpolation of u_h. The interpolation points are represented in red.

to be performed before the numerical integration of the SDE. We choose to exploit the grid defined by Δ_A, interpolating the values of u_h in the center of each square (Figure 13). Let us denote by Q the set of the interpolation points, whose elements are defined by

$$\{Q\}_{ij} = \left(-1 + (i - 0.5)\Delta_A, \quad -1 + (j - 0.5)\Delta_A\right)^T, \quad i, j = 1, \ldots, \frac{2}{\Delta_A} =: N_A. \quad (45)$$

We compute two matrices U_x, U_y of $\mathbb{R}^{N_A \times N_A}$ containing the values of the two components of u_h interpolated on the points of Q. Then, the velocity field is considered to be piecewise constant in each square of the grid defined by Δ_A. Therefore, if we denote by $\tilde{u}$ the transport field for the SDE, at the i-th step of the integration $\tilde{u}$ is evaluated as follows

$$\tilde{u}(X_h(t_i)) = \begin{pmatrix} U_x(\lceil (X_{h,1}(t_i) + 1)/\Delta_A \rceil, \lceil (X_{h,2}(t_i) + 1)/\Delta_A \rceil) \\ U_y(\lceil (X_{h,1}(t_i) + 1)/\Delta_A \rceil, \lceil (X_{h,2}(t_i) + 1)/\Delta_A \rceil) \end{pmatrix}, \quad (46)$$

where $X_{h,1}, X_{h,2}$ denote the first and second components of X_h and $U_x(i, j)$ represents the element (i, j) of the matrix U_x (respectively U_y). Then, given the step size h, one step of DEM will be defined as

$$X_h(t_{i+1}) = \tilde{u}(X_h(t_i))h + \sigma(W(t_{i+1}) - W(t_i)). \quad (47)$$

Given an input initial value X_0 for (42), we approximate the solution using DEM and CEM using the strategy above. In Figure 14 we display 15 trajectories for $X_0 = (-0.8, -0.8)^T$ with two different timesteps. The choice of the initial point is made in order to observe reflections on the lower boundary of the domain D on which we compute the solution, as well as the killing boundary at the right side.
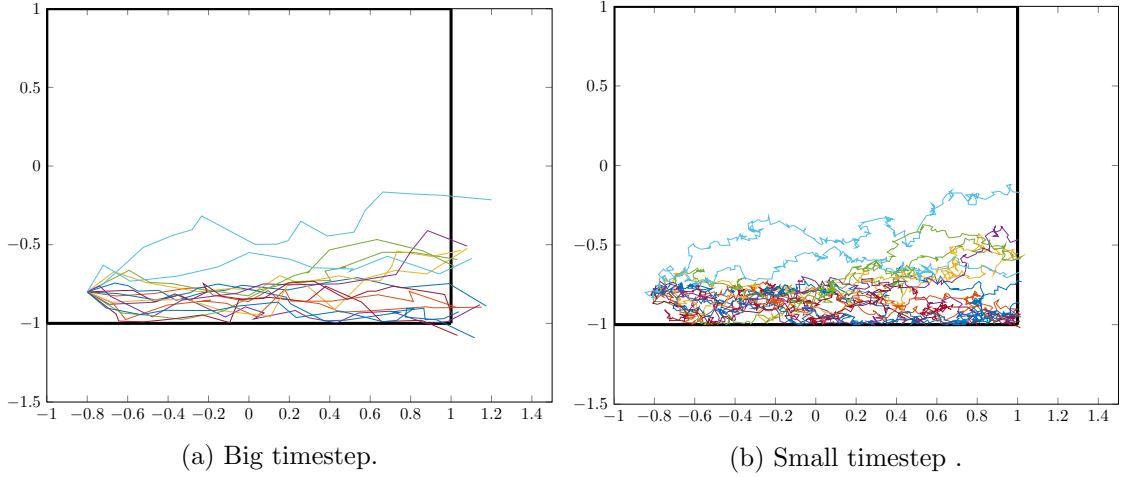
(a) Big timestep.　　　　　　　　(b) Small timestep .

Figure 14: Trajectories of the numerical solution of (42) with DEM.

2.4 Numerical Experiment - Convergence of the method

The method we presented above can lead to incorrect solutions if one of the two parameters Δ_A and h, the timestep chosen for the integration of the SDE (42) with DEM or CEM, is not small enough. Therefore, we perform numerical experiments in order to have an inspect on the convergence of the expected exit time from the domain D. Let us consider the equation (41), with parameters $\sigma_A = 1, \nu = 0.5, L_c = 0.05$ for (44). We generate the random field A and find the pressure and velocity fields using the FEM solver `FreeFem++`. We consider the value Δ_A to be an input parameter for our simulation. Then, we interpolate the retrieved velocity feld as descripted above, and perform a Montecarlo simulation to get a numerical expectation of τ. In order to verify convergence, we vary separately the two parameters of interest, *i.e.*, we will consider h and Δ_A to be fixed alternatively. Let us remark that in order to have a consistent comparison, the values of the exit time have to be estimated using the same realization of A, restricted on a coarser grid if the scope is testing a larger value of Δ_A.

First experiment. Let us consider the final time $T = 10$ and $\sigma = 0.3$ in equation (42), and a Montecarlo simulation over $M = 100000$ trajectories. In Figure 15, the values of the expected exit time for $\Delta_A = 0.5, 0.0625, 0.0078, h_i = T/N_i, N_i = 2^i, i = 0, 1, \dots, 7$ are displayed. It is possible to notice that the results for the fine and the medium grids are approximatively equal, while for the coarse grid the expected exit time do not converge to the same value.
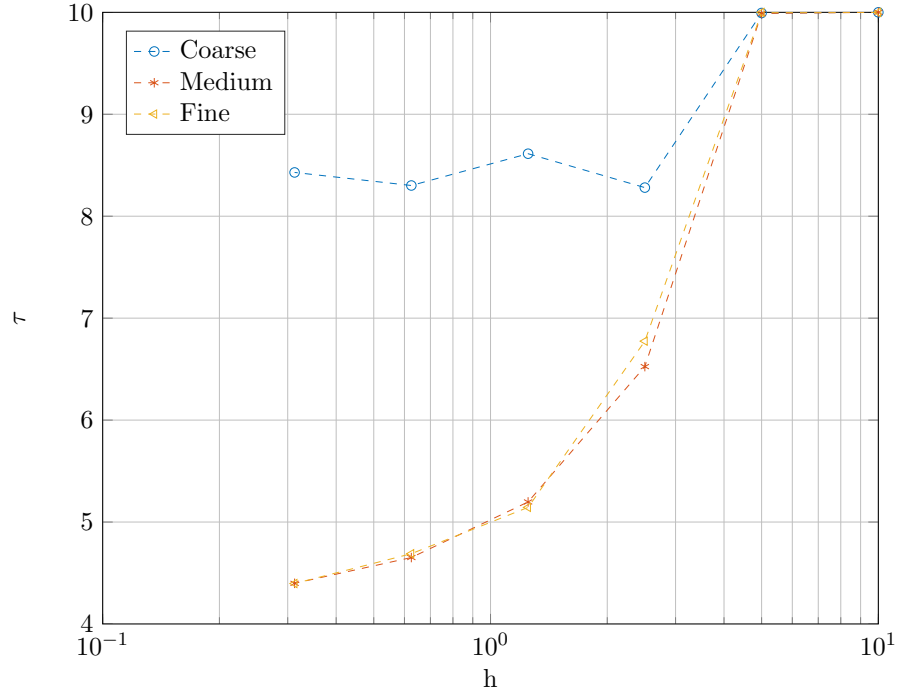
Figure 15: Results for three values of Δ_A (coarse, medium, fine) and convergence with respect to h of the mean exit time.

References

[1] E. Gobet, *Weak approximation of killed di usion using Euler schemes*, Stochastic Processes and their Applications, 87 (2000), pp. 167–197.

[2] E. Gobet, *Euler schemes and half-space approximation for the simulation of diffusion in a domain*, ESAIM: Probability and Statistics, 5 (2001), pp. 261–297.

[3] E. Gobet and S. Menozzi, *Stopped diffusion processes: boundary correction and overshoot*, Stochastic Processes and their Applications, 120 (2010), pp. 130–162.

[4] D. S. Grebenkov and R. Voituriez, *Exit time distribution in spherically symmetric two-dimensional domains*, (2014), pp. 1–34.

[5] D. J. Higham, X. Mao, M. Roj, Q. Song, and G. Yin, *Mean Exit Times and the Multilevel Monte Carlo Method*, SIAM/ASA Journal on Uncertainty Quantification, 1 (2013), pp. 2–18.

[6] S. Krumscheid, M. Pradas, G. A. Pavliotis, and S. Kalliadasis, *Data-driven coarse graining in action: Modeling and prediction of complex systems*, Physical Review E, 92 (2015), p. 042139.

[7] F. Nobile and F. Tesei, *A Multi Level Monte Carlo method with control variate for elliptic PDEs with log-normal coefficients*, Stochastic Partial Differential Equations: Analysis and Computations, (2015), pp. 1–47.

[8] G. A. Pavliotis, *Stochastic Processes and Applications*, 2014.

[9] L. Sirovich, J. E. Marsden, and S. S. Antman, *Theory and Applications of Stochastic Processes: An Analytical Approach*, vol. 170, Springer, 2010.